

**Pharmacodynamic and pharmacokinetic characterization of the aldosterone synthase inhibitor FAD286 in two rodent models of hyperaldosteronism: comparison with the 11 $\beta$ -hydroxylase inhibitor metyrapone**

Dean F. Rigel, Fumin Fu, Michael Beil, Chii-Whei Hu, Guiqing Liang, and Arco Y. Jeng

Cardiovascular and Metabolism Research (DFR, FF, MB, CH, AYJ), Novartis Institutes for BioMedical Research, Novartis Pharmaceuticals Corporation, East Hanover, NJ and Metabolism and Pharmacokinetics (GL), Novartis Institutes for BioMedical Research Cambridge, MA

**Running Title: FAD286 and metyrapone in rat hyperaldosteronism models**

Address for correspondence:

Dean F. Rigel, Ph.D.

One Health Plaza

Building 437/3321

Novartis Institutes for BioMedical Research

Novartis Pharmaceuticals Corporation

East Hanover, NJ 07936-1080

[dean.rigel@novartis.com](mailto:dean.rigel@novartis.com)

Phone: 862-778-0450

FAX: 973-781-5023

|                                  |      |
|----------------------------------|------|
| Number of text pages:            | 24   |
| Number of tables:                | 3    |
| Number of figures:               | 7    |
| Number of references             | 40   |
| Number of words in Abstract:     | 249  |
| Number of words in Introduction: | 694  |
| Number of words in Discussion:   | 1453 |

Nonstandard abbreviations:

ACTH—adrenocorticotrophic hormone

ANG II—angiotensin II

JPET #167148

- 3 -

ASI—aldosterone synthase inhibitor

BAV—bioavailability

CHF—congestive heart failure

CL—clearance

FAD—FAD286

LLOQ—lower limit of quantification

MET—metyrapone

MOH—metyrapol

MRA—mineralocorticoid receptor antagonist

PAC—plasma aldosterone concentration

PCC—plasma corticosterone concentration

PK--pharmacokinetic

RAS—renin-angiotensin system

$t_{1/2}$ —terminal elimination half-life

TWA—time-weighted average

$V_{ss}$ —steady-state volume of distribution.

Recommended section assignment:

Cardiovascular

## ABSTRACT

Aldosterone synthase (CYP11B2) inhibitors (ASI) represent an attractive therapeutic approach for mitigating the untoward effects of aldosterone. We characterized the pharmacokinetic/pharmacodynamic relationships of a prototypical ASI FAD286 (FAD) and compared these profiles to the “11 $\beta$ -hydroxylase inhibitor” metyrapone (MET) in two rodent models of secondary hyperaldosteronism and corticosteronism. In chronically cannulated Sprague-Dawley rats, angiotensin II (ANG II, 300 ng/kg bolus + 100 ng/kg/min infusion) or adrenocorticotrophic hormone (ACTH, 100 ng/kg + 30 ng/kg/min) acutely elevated plasma aldosterone concentration (PAC) from ~0.26 nM to a sustained level of ~2.5 nM for 9 h. ACTH but not ANG II elicited a sustained increase in plasma corticosterone concentration (PCC) from ~300 nM to ~1340 nM. After 1 h of Ang II or ACTH infusion, FAD (0.01-100 mg/kg p.o.) or MET (0.1-300 mg/kg p.o.) dose- and drug-plasma-concentration-dependently reduced the elevated PACs over the ensuing 8 h. FAD was ~12 times more dose-potent than MET in reducing PAC but of similar or slightly greater potency on a plasma drug concentration basis. Both agents also decreased PCC in the ACTH model at relatively higher doses and with similar dose potencies whereas FAD was 6-fold weaker based on drug exposures. FAD was ~50-fold selective for reducing PAC vs. PCC whereas MET was only ~3-fold selective. We conclude that FAD is a potent, orally active, and relatively selective ASI in two rat models of hyperaldosteronism. MET is an order of magnitude less selective than FAD but is, nevertheless, more potent as an ASI than as an 11 $\beta$ -hydroxylase inhibitor.

## INTRODUCTION

Aldosterone is not only a major regulator of extracellular fluid volume and electrolytes but is also linked to the pathogenesis of hypertension and congestive heart failure (CHF) (Weber, 2001; Rocha and Funder, 2002). Aldosterone (mineralocorticoid) receptor antagonists (MRAs), such as spironolactone (Aldactone®) and eplerenone (Inspra®), exhibit antihypertensive, cardiac antihypertrophic, and antiinflammatory properties, organ protection, and reduction of mortality in CHF patients on standard therapies (Pitt, et al., 1999; Fiebeler, et al., 2005; Funder, 2006; Cohn and Colucci, 2006; Fiebeler, et al., 2007).

An alternative therapeutic approach to prevent the deleterious effects of aldosterone is to suppress its production with inhibitors (ASI) of aldosterone synthase (CYP11B2), which catalyzes the final steps of aldosterone biosynthesis (Menard and Pascoe, 2006; Funder, 2006). However, the preferred mechanism to block aldosterone's effects is unknown. ASIs reduce aldosterone and thereby mitigate both its MR- and non-MR-mediated actions (Fiebeler, et al., 2005; Connell and Davies, 2005; Menard, et al., 2006; Marney and Brown, 2007). MRAs can elevate circulating and tissue levels of aldosterone, which may amplify the untoward effects of this steroid mediated by MR-independent pathways (Connell and Davies, 2005; Marney and Brown, 2007). In contrast, treatment with an ASI could allow activation of the unprotected MR by glucocorticoids (Funder, 2009). Resolution of this debate has been hindered by the limited availability of potent, effective, selective, and orally active ASIs.

FAD286 (CGS020286A; FAD) is a prototypical ASI that has undergone limited *in vivo* preclinical testing (Fiebeler, et al., 2005; Lea, et al., 2009; Menard, et al., 2006; Minnaard-Huiban, et al., 2008; Mulder, et al., 2008) and has been recommended for clinical evaluation (Menard and Pascoe, 2006; Funder, 2006; Siragy and Xue, 2008). FAD is the R(+)-enantiomer of the racemic

CYP19 (aromatase) inhibitor CGS016949A (fadrozole, Afema®), which is marketed in Japan as a treatment for estrogen-dependent breast cancer. Although its antipode is an aromatase inhibitor, FAD potently inhibits human AS *in vitro* (Fiebeler, et al., 2005;Muller-Vieira, et al., 2005;Mulder, et al., 2008;LaSala, et al., 2009). Its potency against AS from non-human species is unknown. Likewise, clinical evaluation of FAD has not been reported. However, at or somewhat above marketed doses, the racemate fadrozole lowers basal or stimulated plasma aldosterone in humans (Stein, et al., 1990;Dowsett, et al., 1990;Trunet, et al., 1992). FAD also lowers plasma aldosterone concentration or urinary aldosterone excretion in transgenic or genetic rat models of hypertension or heart failure (Fiebeler, et al., 2005;Menard, et al., 2006;Minnaard-Huiban, et al., 2008).

The optimal dose of FAD for inhibiting aldosterone production in rats is unknown. In a transgenic rat model of angiotensin II (ANG II)-dependent hypertension, 3.4 mg/kg/day of FAD free base exhibited cardiac and renal protection and reduced the post-weaning rise in blood pressure compared with untreated controls (Fiebeler, et al., 2005). Adrenalectomy reduced serum and cardiac aldosterone levels considerably more than did FAD and further ameliorated the cardiac and renal injury, suggesting that the utilized dose of FAD (Lea, et al., 2009) was submaximal. This notion is supported by a study in spontaneously hypertensive rats in which 86 mg/kg/day (100 mg/kg of the HCl salt) of FAD was required to maximally lower 24-h urinary aldosterone excretion (Menard, et al., 2006). None of these studies could determine the time course of aldosterone reduction or the pharmacokinetics of FAD since only a single terminal blood sample was withdrawn or the time-integrated urinary aldosterone excretion was measured. Likewise, the FAD exposure-response relationships and the extent of CYP11B1 (11β-

hydroxylase) inhibition and, thus, the lowering of corticosterone at optimal therapeutic doses of FAD are unclear (Fiebeler, et al., 2005;Lea, et al., 2009;Minnaard-Huiban, et al., 2008).

The purpose of this study was several-fold: 1) to develop facile and robust ASI profiling models in rats; 2) to use these models to characterize the dose-dependent magnitude and duration of action of FAD *in vivo*, 3) to assess the PK/PD relationships and traditional PK parameters of FAD *in vivo*, 4) to evaluate the CYP11B2/CYP11B1 selectivity of FAD *in vivo*, and 5) to compare these *in vivo* results with *in vitro* potency/selectivity profiles in a rat adrenal cortical CYP11B2/CYP11B1 preparation. Furthermore, these profiles of the CYP11B2 inhibitor FAD were compared with those of metyrapone (MET; Metopirone®), which has been utilized for many years as a CYP11B1 inhibitor for clinical diagnosis and treatment of hypothalamic-pituitary-adrenal axis disorders.

## MATERIALS AND METHODS

### **In vivo Experiments**

#### **Animal Use**

All animal procedures were conducted in accordance with an approved Institutional Animal Care and Use Committee protocol and the Guide for the Care and Use of Laboratory Animals.

Experiments were conducted on 121 male, adult, Sprague-Dawley rats (mean body weights 517 g (range 404-715 g)) purchased from Taconic Farms (Germantown, NY). After arrival to the Novartis vivarium, rats were acclimated for at least several weeks before being used in the experiments. They were housed on a 12-h light/dark cycle (light: 6 am to 6 pm) at temperature and relative humidity set points of 72°F and 55%, respectively. Rats were provided normal chow (Harlan Teklad 8604; Indianapolis, IN) and water ad libitum except for a partial fast before and during each experiment, in which case, all but two chow pellets were removed the preceding evening (~5 pm). On the morning of the experiment, any remaining food was removed. Food was again provided ad libitum at the experiment terminus.

#### **Surgical Instrumentation**

Rats were surgically instrumented to allow direct measurement of arterial blood pressure, repeated blood sampling, and intravenous (i.v.) or intra-arterial (i.a.) administration of substances. Under isoflurane anesthesia, a femoral artery and vein were isolated and catheterized. Catheters consisted of 55 cm of Tygon® (PVC) microbore tubing (0.020" I.D X 0.060" O.D.) bonded with cyclohexanone to 4.5 cm of polyvinylchloride (0.011" I.D. X 0.024" O.D.; Biocorp Australia Pty Ltd, Huntingdale, Vic., Australia) or Micro-Renathane (Type MRE-025 polyurethane; 0.012" I.D. X 0.025" O.D.; Braintree Scientific Inc., Braintree, MA) tubing. The catheters were tunneled subcutaneously and exteriorized in the mid-dorsal



thoracic/abdominal region. Catheters exited through a subcutaneously anchored tether/swivel system that allowed the animal to move unrestrained in a specialized plastic wire-bottom cage. Ketoprofen (1 mg/kg i.m.) was administered for pre-emptive analgesia before beginning the surgical procedure and again on the first post-operative day. Also, penicillin G (50,000 U/kg i.m.) was administered pre-operatively to prevent infection. The rats were allowed to recover for a minimum of one week before being studied while conscious and unrestrained. Catheters were flushed with sterile 0.9% saline and locked with 200 U/ml heparin in sterile 0.9% saline after the surgery was completed and at least twice per week thereafter.

### **Experimental Procedures**

Rats were allowed to remain undisturbed in their home cages before, during, and after each experiment. On the morning of the study, the catheters were flushed and prepared for use. In some experiments, arterial pressure was monitored via the arterial catheter, a calibrated blood pressure transducer (P23, Statham), and a digital data acquisition system (Modular Instruments, Inc., Westchester, PA).

Blood samples were withdrawn on heparin (15 U/ml final concentration) from the arterial cannula. Samples were centrifuged at 20000g for ~20 minutes to generate plasma, which was aliquoted and frozen (-70°C) for later analysis of plasma aldosterone (PAC), corticosterone (PCC), or drug concentrations.

ANG II or ACTH was infused into the venous catheter. FAD, MET, or vehicle were administered as a bolus i.a. or by oral gavage.

### **Experimental Protocols**

Infusion doses of ANG II and ACTH were determined from pilot dose-response experiments (ANG II: 3-100 ng/kg/min; ACTH: 0.3-300 ng/kg/min). The final doses (see below) were

selected to achieve sustained increases in PAC to the target level of 1-5 nM (360-1800 pg/ml). These PACs represent the middle- to upper-range reported in patients with primary aldosteronism (Phillips, et al., 2000;Perschel, et al., 2004;Unger, et al., 2004). Rats with baseline PAC values outside this range were excluded from analyses (see Results). Most doses of ANG II also elevated mean arterial pressure by ~40 mmHg whereas ACTH had no evident effect on blood pressure.

The final dosing regimens selected for the experiments were bolus injections (ANG II, 300 ng/kg; ACTH, 100 ng/kg) followed by a 9-h i.v. infusion (100 or 30 ng/kg/min, for ANG II or ACTH, respectively). In some studies, pre-ANG II or ACTH blood samples were withdrawn. After 1 h of ANG II or ACTH infusion, a blood sample was collected for determining the post-ANG II or ACTH “baseline” (i.e., secretagogue-elevated) PAC and PCC. FAD (0.01-100 mg/kg p.o.; 1 mg/kg i.a.), MET (0.1-300 mg/kg; 10 mg/kg i.a.), vehicle, or no treatment was administered, and the ANG II or ACTH infusion was continued for an additional 8 h. Blood samples were withdrawn at 5 (i.a. dosing only), 15, and 30 min, and 1, 2, 3, 4, 5, 6, 7, 8, and 24 h post-dosing for assessment of PAC, PCC, and plasma drug concentrations.

Some of the ANG II-treated rats were used for more than one experiment after allowing at least one week of recovery from the previous experiment. Model validation experiments confirmed that results with this experimental paradigm were highly reproducible. In contrast, in rats administered ACTH, corticosteroid responses to a second ACTH infusion were not reproducible even after several weeks of recovery from the initial experiment. Therefore, rats receiving ACTH were used for only one experiment and then euthanized.

### **In vitro Experiments**

#### **Rat adrenal tissue CYP11B1 and CYP11B2 assays**

Male Sprague-Dawley rats were anesthetized with isoflurane and both adrenal glands were surgically removed. The glands were decapsulated and the capsular tissue frozen in liquid nitrogen and stored at  $-80^{\circ}\text{C}$ . Thawed adrenal capsules were pooled and homogenized in 1 ml of ice-cold homogenization buffer (8.5 mM  $\text{MgCl}_2$ , 3.13 mM KCl, 7.59 mM NaCl, 2.7 mM  $\text{CaCl}_2$ , 50 mM Tris/HCl, pH 7.4, and one Complete<sup>TM</sup> EDTA-free Protease Inhibitor Cocktail Tablet (Roche Applied Science, Indianapolis, IN) per 50 ml buffer) per 37.5 mg tissue. The homogenized material was then centrifuged at 450 x g for 5 min, and the supernatant was collected. The supernatant was brought to a final glycerol concentration of 5%, flash-frozen in liquid nitrogen, and stored at  $-80^{\circ}\text{C}$ .

Material from frozen adrenal homogenate preparations was thawed on ice on the day of experiment and then diluted in ice-cold assay buffer (8.5 mM  $\text{MgCl}_2$ , 3.13 mM KCl, 7.59 mM NaCl, 2.7 mM  $\text{CaCl}_2$ , and 50 mM Tris/HCl, pH 7.4) to a protein concentration of approximately 3 mg/ml. The CYP11B1 and CYP11B2 assays were performed in white 96-well clear, flat-bottom, non-treated, assay plates. For the CYP11B1 assay, 1 to 2  $\mu\text{g}$  of protein in 20  $\mu\text{l}$  was incubated with 10  $\mu\text{l}$  of assay buffer or a compound at the desired concentration and 20  $\mu\text{l}$  of substrate mix (2.5x NADPH Regeneration Solution A, 2.5x NADPH Regeneration Solution B, 1.25  $\mu\text{M}$  11-deoxycorticosterone) for 4 h at  $25^{\circ}\text{C}$  in a shaking incubator. Final substrate concentration was 0.5  $\mu\text{M}$ . The reaction was stopped by freezing the plates over dry ice. Production of corticosterone was measured by scintillation proximity assay (SPA).

The CYP11B2 assay was carried out similarly, except that 15 to 20  $\mu\text{g}$  of protein and 1  $\mu\text{M}$  11-deoxycorticosterone (final concentration) were used. Production of aldosterone was also determined by SPA.

Measurement of aldosterone and corticosterone was performed using a 96-well-plate format. Test samples were incubated with 0.02  $\mu\text{Ci}$  of either D-[1,2,6,7- $^3\text{H}(\text{N})$ ]corticosterone (CYP11B1) or D-[1,2,6,7- $^3\text{H}(\text{N})$ ]aldosterone (CYP11B2) and 0.2  $\mu\text{g}$  of either anti-corticosterone or anti-aldosterone antibody in PBS containing 0.1% Triton X-100, 0.1% bovine serum albumin, and 12% glycerol in a total volume of 200  $\mu\text{l}$  at room temperature for 1 h. Anti-sheep (corticosterone) or anti-mouse (aldosterone) PVT SPA beads (50  $\mu\text{l}$ ) were then added to each well and incubated overnight at room temperature prior to counting in a Microbeta plate counter. The amount of corticosterone or aldosterone in each sample was calculated by comparing with standard curves generated using known quantities of the respective steroid.

Full concentration-response curves of an inhibitor were generated from at least 3 independent experiments.

### **Plasma protein binding assay**

*In vitro* plasma protein binding of FAD, MET, racemic metyrapol, and the two metyrapol enantiomers was assessed in triplicate using an equilibrium dialysis method (Rapid Equilibrium Dialysis (RED) System; Pierce Biotechnology, Inc., Rockford, IL). Compound was added to rat or human plasma at a final concentration of 1 or 10  $\mu\text{M}$  (in 1% DMSO). The plasma was incubated at 37°C for 4 h in the RED Device. Parent compound concentrations in the plasma and phosphate-buffered saline (PBS) compartments were measured at time 0 and 4 h by LC/MS/MS. Percent of parent compound bound in plasma and percent recovery were calculated as:

$$\% \text{ Bound} = (1 - ([\text{PBS}]_{4\text{h}}/[\text{Plasma}]_{4\text{h}})) \times 100\%$$

$$\% \text{ Recovery} = (([\text{PBS}]_{4\text{h}} + [\text{Plasma}]_{4\text{h}})/[\text{Plasma}]_{0\text{h}}) \times 100\%$$

### **Ex vivo Analyses**

PACs and PCCs were assayed with commercially available radioimmunoassay kits (Coat-A-Count Aldosterone, TKAL-4; Coat-A-Count Rat Corticosterone TKRC1; Diagnostic Products Corp., Los Angeles, CA) with unextracted plasma according to the manufacturer's instructions. The intra- and inter-assay CVs were  $\leq 3\%$  for aldosterone and  $\leq 12\%$  for corticosterone.

Plasma concentrations of FAD and MET were measured by an LC/MS/MS method (lower limit of quantification (LLOQ) = 0.5 ng/ml = 2.24 nM and 1 ng/ml = 4.4 nM, for FAD and MET, respectively). Likewise, the concentrations of the two primary reduced metabolites of MET ((+)- and (-)-MOH) were measured by LC/MS/MS with a Chiral PAK 4.6 x 150 mm chiral column (LLOQ = 1 ng/ml = 4.4 nM). Quantification of the analytes was based on a calibration curve with at least 5 points and a dynamic range set from the respective LLOQs to 10  $\mu\text{g/ml}$ . The bias of all calibration standards and quality control samples was within 30%. In each case, samples with drug concentrations below the LLOQ were treated as zero for computations of means.

### **Drugs and reagents**

Stock solutions of ANG II (A9525; Sigma-Aldrich, St. Louis, MO) and ACTH(1-24) (herein referred to as "ACTH"; product number 10-1-21; American Peptide Company, Inc., Sunnyvale, CA) were prepared in sterile saline or water based on the respective purities and peptide contents stated by the manufactures. Aliquots were frozen at  $-70\text{ }^{\circ}\text{C}$ . On the day of the experiment, an infusion solution was prepared in sterile saline at a calculated concentration (5 and 1.5 ng/ $\mu\text{l}$  for ANG II and ACTH, respectively) to allow an infusion volume of 20  $\mu\text{l/kg/min}$ .

FAD (hydrochloride or hydrogentartrate salt) was synthesized within Novartis (see Fiebeler, et al., 2005 for FAD structure). MET (2-methyl-1,2-di-3-pyridyl-1-propanone, Product #856525) was purchased from Sigma-Aldrich and its primary racemic metabolite (MOH) was generated within Novartis by sodium borohydride reduction of MET (see Nagamine, et al., 1997 for MET

& MOH structures). The (+)- and (-)- enantiomers of MOH were resolved from the racemate by chiral chromatography (CHIRALPAK<sup>®</sup> IA, Daicel Chemical Industries, Ltd., Fort Lee, NJ; mobile phase: 15% Ethanol/Heptane). Formulated FAD and MET were prepared freshly from the powders before each experiment. Vehicles (2 ml/kg volume) were water for p.o. administration or sterile 0.9% saline for i.a. injection. Doses of both salt forms of FAD are reported as mg/kg of the free base of the drug.

NADPH Regeneration Solution A and Solution B were purchased from BD Biosciences Clontech (Palo Alto, CA). Anti-sheep and anti-mouse Amersham PVT SPA beads were acquired from GE Healthcare Life Sciences (Piscataway, NJ). [1,2,6,7-<sup>3</sup>H(N)]Corticosterone and D-[1,2,6,7-<sup>3</sup>H(N)]aldosterone were products of PerkinElmer (Boston, MA).

### **Data and statistical analyses**

For each individual rat, the PAC and PCC time-course data were expressed as a percent of the respective baseline value. For dose- and concentration-response analyses, the “pharmacodynamic response” was defined as the peak lowering of PAC or PCC (“PEAK”) or the time-weighted average of this baseline-normalized PAC and PCC over the 8-h experiment (“TWA” = area under the curve ÷ 8 h). Likewise, the TWAs of the plasma FAD and MET concentrations were estimated from the 8-h AUCs.

ED<sub>50</sub>, EC<sub>50</sub>, and IC<sub>50</sub> values (*in vivo* dose or plasma concentration at 50% of “baseline” response or half-maximally effective *in vitro* concentration) were estimated by fitting the individual dose- or concentration-response data to a 4-parameter sigmoidal dose-response model (Model 205) in XLfit (Version 4, ID Business Solutions, Inc., Guildford, UK):

$$\text{Response} = A + (B - A) / (1 + (C/X)^D)$$

where A and B represent the responses at supramaximally effective and subthreshold concentrations/doses, respectively, C is the concentration/dose that produces a half-maximal response, D is a slope constant, and X is the test concentration or dose.

PK parameters were calculated with the computer program WinNonlin (Enterprise, Version 5.2, Pharsight Corporation, Palo Alto, CA) using a noncompartmental model for the parent drug. PK data were calculated based on individual concentrations. The area under the concentration-time curve (AUC) was calculated using the linear trapezoidal rule. Likewise, the time-weighted average drug concentration, PAC, and PCC were computed as the AUC divided by the integration time (8 h).

Results are presented as mean  $\pm$  SEM. Unpaired t-test (Microsoft Excel) was used to discern statistically significant differences ( $p < 0.05$ ) in values between two experimental groups. One-way ANOVA was applied to determine whether the control PAC and PCC responses were sustained at 100% over the 8-h experiment. Multiple comparisons vs. the time-0 values were conducted with Dunnett's test.

## RESULTS

### **Inhibition of Aldosterone and Corticosterone Production by FAD, MET, and MOH *In vitro***

Aldosterone and corticosterone products were generated time-dependently from the DOC substrate by rat adrenal capsular preparations with respective rates of  $43 \pm 4$  pmol/mg protein/h (mean  $\pm$  SEM,  $n = 4$ ) and  $4.9 \pm 0.5$  nmol/mg protein/h up to 4 h (results not shown). These results show that corticosterone is produced at a rate about 2 orders of magnitude greater than that of aldosterone.

All four compounds dose-dependently inhibited biosynthesis of aldosterone (CYP11B2) and corticosterone (CYP11B1) *in vitro* (Fig. 1). FAD, MET, and (+)-MOH exhibited a similar potency against CYP11B2 whereas (-)-MOH was ~6-7 times less potent (Table 1). MET was the most potent compound against CYP11B1 but was, nevertheless, 2 times more selective for CYP11B2 than CYP11B1. (-)-MOH was equipotent against both enzymes whereas FAD and (+)-MOH were 5- and 4-fold more selective, respectively, for CYP11B2 (Table 1).

### **Inhibition of Aldosterone and Corticosterone Production by FAD and MET *In vivo***

One-hundred forty-eight experiments were conducted on 121 rats. Of these, six were excluded from the analyses because the baseline PAC deviated from the target range of 1-5 nM and one was excluded because of technical problems.

#### **Basal and Baseline PACs and PCCs**

Before administration of ANG II or ACTH, the basal PAC and PCC values were ~0.28 nM and ~300 nM, respectively, reflecting the expected ~3 order-of-magnitude-higher levels of glucocorticoid than mineralocorticoid. ANG II and ACTH bolus/infusions rapidly increased PACs and PCCs, which reached a steady-state within 1 h ("baseline" PAC or PCC (i.e., "time 0")). These baseline values were similar for all treatment groups (PAC, ~2.5 nM; PCC, ~1300



nM). Thus, the secretagogues elevated PAC and PCC by ~10-fold and ~4- to 5-fold, respectively, over basal levels (results not shown).

### **Time courses of PAC and PCC in the Control experiments with ANG II and ACTH**

Each rat's PAC and PCC time-course data were normalized to its own baseline PAC or PCC by expressing the results as a percent of the baseline value. Responses in untreated and vehicle-treated control rats were similar and therefore combined for each secretagogue. Infusion of ANG II in control rats resulted in a sustained increase in PAC (~100%) for at least 9 h (Fig. 2). In contrast, PCC remained elevated for only the first 2 h and then significantly declined ( $P=0.001$ ) at 3 h to achieve a steady-state of 50% by 5 h. Because of this transient increase in PCC, the ANG II model was used to evaluate the effects of the pharmacologic agents on only PAC. ACTH maintained the stimulated level of both PAC and PCC at ~100% and was, therefore, used to evaluate the PAC/PCC selectivity of the inhibitors.

### **PAC and PK time-course responses to FAD and MET in the ANG II model**

Fig. 3 displays the PAC time-courses as percent of baseline PAC (mean  $\pm$  SEM) for each of the p.o. doses of FAD (upper-left panel) and MET (upper-right panel) as well as the plasma compound concentrations (lower panels) in the ANG II-infused rats.

FAD dose- and time-dependently lowered PAC. At the two lowest doses of FAD, PAC was transiently elevated above baseline followed by a ~20% decrease and then a recovery. All of the remaining doses elicited a sustained, dose-dependent decrease in PAC for the duration of the experiment. The maximally effective dose appeared to be 3-10 mg/kg. At doses of 1 mg/kg and higher, PAC declined with a characteristic temporal pattern over the first 2-3 h post-dosing.

MET also dose- and time-dependently lowered PAC in this model. At the two lowest doses, the reduction of PAC was transient and followed by a rebound above the baseline. Likewise, at

doses of 1-10 mg/kg, the PAC began to recover after ~5 h. In contrast, the two highest doses of MET decreased PAC for the duration of the 8-h experiment. Interestingly, the pattern of PAC decline during the first 2-3 h was almost identical to that of FAD. This common profile suggests that it is attributable to the intrinsic metabolism/elimination characteristics of aldosterone and not to the tissue-distribution and enzyme-kinetic properties of the two compounds.

Oral treatment with FAD dose- and time-dependently elevated plasma FAD concentrations (Fig. 3). Plasma FAD concentrations were nearly constant throughout the 8-h experiment whereas MET levels declined by ~an order of magnitude. Twenty-four hours after dosing, plasma concentrations decreased even more for MET compared to FAD.

#### **PAC, PCC, and PK time-course responses to FAD and MET in the ACTH model**

Fig. 4 displays the time-courses of PAC and PCC as a percent of the respective baseline values (mean  $\pm$  SEM) for each of the p.o. doses of FAD (two upper-left panels) and MET (two upper-right panels) and the plasma compound concentrations (lower panels) in the ACTH-infused rats.

As in the ANG II model, both FAD and MET dose- and time-dependently lowered PAC. One striking difference, however, was the shorter duration of action and overshoot above baseline in PAC at the low-to-moderate doses of FAD and MET. This effect was not evident with PCC. The reason for this difference is not clear. However, pilot experiments with renin-angiotensin system (RAS) blockade suggest that this pattern was not due to ASI-induced counter-regulatory activation of the RAS, which was intact in the ACTH model but “clamped” in the ANG II-infusion model. Accordingly, it appears as though higher doses of FAD or MET were required to elicit a comparable PAC response to that in the ANG II model or to yield a sustained lowering of PAC. Again, the characteristic pattern of the decline in PAC during the first 2-3 h after FAD or MET was similar to that in the ANG II model.

Oral treatment with FAD and MET dose- and time-dependently elevated plasma compound concentrations similar to those in the ANG II model.

### **Dose-response relationships of FAD and MET in the ANG II and ACTH models**

The “PD responses” for FAD and MET were derived as the peak (Fig. 5, upper panels) or TWA (Fig. 5, lower panels) of the baseline-normalized PAC or PCC over the 8-h experiment. In the control (“C”) experiments (grey symbols in Fig. 5), there was no net effect on PAC or PCC in the two models.

FAD and MET dose-dependently lowered peak and TWA PAC and PCC (Fig. 5). Both compounds tended to be less potent in lowering PAC in the ACTH model (i.e., rightward shift in dose-response relationships) than in the ANG II model. This is consistent with the observation that the magnitude and duration of PAC lowering was attenuated in the ACTH model compared to the ANG II model (*cf.* 3, 4 and 4). Both FAD and MET were more potent in lowering PAC than PCC in the ACTH model (Fig. 5). Thus, FAD is a relatively selective ASI whereas MET is clearly not a selective 11 $\beta$ -hydroxylase inhibitor in this model. Note that these *in vivo* rat PAC/PCC results reflect the relative CYP11B2/CYP11B1 profiles observed in the *in vitro* rat adrenal cortical assays (Fig. 1). Likewise, both compounds tended to be more efficacious in lowering PAC than PCC (Fig. 5).

### **Dose-exposure relationships of FAD and MET in the ANG II and ACTH models**

Oral administration of FAD and MET dose-dependently elevated the plasma concentrations of the respective parent compounds (Fig. 6). Exposures were similar between the two models at the highest doses but tended to be slightly higher in the ACTH model at the lowest doses tested. Peak concentrations of both compounds increased dose-proportionally. Eight-hour TWA

concentrations of FAD tended to increase dose-overproportionally whereas those for MET increased dose-proportionally.

After i.a. administration of FAD (1 mg/kg), the 8-h TWA plasma concentrations of FAD were similar to those after the same p.o. dose (Fig. 6, lower panel), suggesting a relatively high oral bioavailability (BAV) for this compound. In contrast, there was a greater separation between the i.a. (10 mg/kg) and p.o. exposures of MET, indicating a lower oral BAV (see PK results below).

### **Exposure-response relationships of FAD and MET in the ANG II and ACTH models**

The exposure-response relationships (Fig. 7) were derived by combining the dose-response (Fig. 5) and dose-exposure (Fig. 6) relationships. FAD and MET concentration-dependently lowered PAC and PCC. As described for the dose-response relationships, both compounds tended to be less potent in lowering PAC in the ACTH model than in the ANG II model. This pattern is particularly striking for the 8-h TWA for MET due to the shorter duration of action in the ACTH model. As observed for the dose-response relationships (Fig. 5), both FAD and MET were also more potent on a plasma exposure basis in lowering PAC than PCC in the ACTH model (Fig. 7).

### **ED<sub>50</sub>, EC<sub>50</sub> (total and unbound), and PAC/PCC selectivity values *in vivo***

ED<sub>50</sub> and EC<sub>50</sub> values for lowering PAC and PCC in the two models are displayed in Table 2. FAD was ~12 times (i.e., ED<sub>50</sub> values = 0.5 vs. 5.5 mg/kg in the ANG II model and 0.8 vs. 10.6 mg/kg in the ACTH model) more potent than MET on a dose basis in reducing PAC of similar potency on a plasma drug concentration basis. In the ACTH model, both agents also decreased PCC at relatively higher doses and with similar dose potencies (ED<sub>50</sub> values = 45 vs. 40 mg/kg), whereas FAD was 6-fold weaker than MET based on drug exposures (EC<sub>50</sub> values = 23000 vs. 3600 nM). Accordingly, based on both ED<sub>50</sub> and EC<sub>50</sub> values, FAD was ~50-fold selective for reducing PAC than PCC but MET was only ~3-fold selective.

*In vitro* protein binding in rat and human plasma was low and similar for FAD and MET (rat: FAD, 57%; MET, 33%; human: FAD, 55%; MET, 27%). Likewise, plasma protein binding for the MOH enantiomers were nearly identical to those of MET. Thus, the “unbound” EC<sub>50</sub> values for FAD and MET were ~43% and 67%, respectively, of the “total” EC<sub>50</sub> values (Table 2) and FAD was only slightly (1.6-fold = 67%/43%) more potent than MET based on unbound concentrations relative to the total concentration EC<sub>50</sub> values.

#### **(+)- and (-)-MOH concentrations in the ANG II and ACTH models**

At each MET dose, individual-time, peak, and 8-h TWA concentrations of (-)-MOH were ~3-10 times higher than the corresponding (+)-MOH levels (Supplemental Fig. S1, upper-right vs. upper-left panel), indicating an enantioselective generation and/or metabolism of the two MOH metabolites. Concentrations of (+)- or (-)-MOH equaled or exceeded those of MET at the 3-5 highest doses of MET (Supplemental Fig. S1, Supplemental Fig. S2).

Based on the relative *in vitro* potencies of MET and its two metabolites (Table 1) and the relative *in vivo* concentrations of each (Fig. 6 and Supplemental Fig. S1), we estimated the contributions of (+)- and (-)-MOH to the overall pharmacodynamic response of p.o.-administered MET (30-300 mg/kg). These calculations suggest that the combined (+)- and (-)-MOH effect on PAC and PCC was 4-6 and 4-7 times higher, respectively, than that of MET alone, indicating the important pharmacologic contribution of these active metabolites.

#### **PK parameters**

Oral BAV of FAD increased dose-dependently and ranged from 16% to 100% depending on the model and dose (Supplemental Fig. S3, left panel). Oral BAV for MET was low (~10%), independent of dose, and similar between the two models (Supplemental Fig. S3, right panel).

JPET #167148

- 22 -

PK parameters (Table 3) were similar between the two models for both compounds. The only exception was clearance (CL), which was significantly higher (~2-fold) for FAD in the ACTH model than in the ANG II model. Also, the elimination half-life of MET was significantly longer than that of FAD in the ACTH model and the  $V_{ss}$  was significantly higher for MET than FAD in both models.

## DISCUSSION

Pharmacologic suppression of aldosterone synthesis with ASIs is an attractive therapeutic alternative to MRAs. However, appropriate *in vivo* models for pharmacologically characterizing such agents are uncommon (Fiebeler, et al., 2005;Menard, et al., 2006). MRAs have traditionally been evaluated by assessing urinary electrolytes or organ injury in rodent models with *exogenously* administered aldosterone (Rudolph, et al., 2004;McManus, et al., 2008;Brandish, et al., 2008). In contrast, profiling ASIs requires stimulation of *endogenous* aldosterone production either by pharmacologic or dietary activation of biosynthetic pathways (Rowland and Morian, 1999;Ye, et al., 2003;Menard, et al., 2006), exogenous administration of natural or synthetic secretagogues for corticosteroids (Komor and Muller, 1979;Lea, et al., 2009;Mazzocchi, et al., 1989;Roesch, et al., 2000;Ye, et al., 2003), or transgenic manipulations (Sander, et al., 1992;Garnier, et al., 2004;Fiebeler, et al., 2005;Makhanova, et al., 2008).

Our first goal was to develop a model of hyperaldosteronism in conscious, chronically cannulated rats to simultaneously assess the PD and PK profiles and corticosteroid selectivity of ASIs. We sought to increase PAC to the middle- to upper-range (1-5 nM = 360-1800 pg/ml) reported in patients with primary hyperaldosteronism (Phillips, et al., 2000;Perschel, et al., 2004;Unger, et al., 2004). Initially, we explored low-sodium diet, dietary potassium supplementation, diuretic/natriuretic treatment, or combinations thereof to amplify endogenous aldosterone. Although each of these strategies was effective (Rowland and Morian, 1999;Ye, et al., 2003;Menard, et al., 2006), the resultant PAC increases were gradual, highly variable, and not temporally stable over a single- or multiple-day study. Moreover, these interventions exaggerated diurnal variations in corticosteroid levels and stress responses to oral gavage and generated no or small elevations in corticosterone (Rowland and Morian, 1999;Ye, et al., 2003).

Together, these factors greatly limited the utility of these approaches. In contrast, continuous intravenous infusion of either of the primary aldosterone secretagogues (ANG II or ACTH) overcame these limitations; PAC was consistently elevated to a steady level for at least 8 h. ACTH infusion also stably increased corticosterone thereby allowing simultaneous evaluation of the CYP11B2/CYP11B1 selectivity of the compounds.

In both models, FAD dose- and concentration-dependently attenuated the secretagogue-elevated PAC. This inhibitory response was sustained for at least 8 h at doses  $\geq 1$  mg/kg. The maximally effective dose (~3-30 mg/kg) within this time window depended on the “response” (peak or 8-h TWA) and the model (ANG II or ACTH). Doses required to block AS for 24 h might be even higher. Indeed, in spontaneously hypertensive rats, 86 mg/kg/day (100 mg/kg of the HCl salt) of FAD was needed to maximally lower 24-h urinary aldosterone excretion (Menard, et al., 2006). Likewise, in a transgenic rat model of ANG II-dependent hyperaldosteronism, 3.4 mg/kg/day (4 mg/kg of the HCl salt) of FAD only partly lowered PAC relative to bilateral adrenalectomy (Fiebeler, et al., 2005). Thus, our comprehensive characterization of FAD is critical for defining the drug’s effective dose range and suggests that its therapeutic benefits were underestimated by studies using suboptimal doses (0.24-3.4 mg/kg/day) (Lea, et al., 2009;Minnaard-Huiban, et al., 2008;Siragy and Xue, 2008;Mulder, et al., 2008).

The effective *in vitro* FAD concentrations appear to reflect the effective plasma exposure-response relationships; the total (120 or 480 nM) and unbound (54 or 210 nM) EC<sub>50</sub> values for reducing PAC in our two models are comparable to the IC<sub>50</sub> (670 nM) for inhibiting CYP11B2 in the rat adrenal homogenate assay. Concentrations at AS within adrenal mitochondria are probably higher than the plasma levels since FAD is preferentially distributed into the adrenal cortical tissue (unpublished observation). Nevertheless, the consistent *in vivo* exposure-response



relationships suggest that the plasma FAD concentrations do predict the extent of PAC suppression in rats and, presumably, in humans or other species.

The effective dose of FAD for lowering PAC in rats appears to be considerably higher than that in humans based on clinical studies with the racemic fadrozole (CGS 16949A). Daily doses of ~4 mg (~0.06 mg/kg) fadrozole suppressed basal and ACTH-stimulated PAC in postmenopausal women with breast cancer or in healthy males (Stein, et al., 1990;Dowsett, et al., 1990;Trunet, et al., 1992). Thus, FAD is several hundred-fold more potent on a body-weight-normalized dose basis in humans than in rats. This *in vivo* species disparity is consistent with the ~20- to 400-fold greater potency of FAD in human adrenocortical carcinoma (NCI-H295R) cells ( $IC_{50} = 37$  nM) and recombinant human AS ( $IC_{50} = 1.6$  nM) (Fiebeler, et al., 2005;LaSala, et al., 2009) versus our  $IC_{50}$  (670 nM) in rat adrenal cortical homogenates.

FAD was 5-fold selective for inhibiting biosynthesis of aldosterone (via CYP11B2) versus corticosterone (via CYP11B1) in our rat adrenocortical assay and similar to its selectivity (6-fold) reported in the recombinant human enzyme preparations (LaSala, et al., 2009). In our rat ACTH model, FAD exhibited 50-fold selectivity for lowering PAC versus PCC on both a dose ( $ED_{50}$ ) and plasma-concentration ( $EC_{50}$ ) basis. This observation suggests that the translation from *in vitro* to *in vivo* conferred to this ASI an additional CYP11B2/CYP11B1 selectivity (~10X). However, we observed no such *in vitro* to *in vivo* amplification for MET, possibly because MET also inhibits the conversion of cholesterol to pregnenolone (Carballeira, et al., 1974), an upstream step that is common to both mineralocorticoid and glucocorticoid biosynthesis. Since our *in vitro* rat adrenal assays utilized the immediate precursor substrate (11-deoxycorticosterone) for the CYP11B2 and CYP11B1 enzymes, this off-target activity of MET would be evident only *in vivo*. Overall, these results indicate the feasibility of developing ASIs

that are relatively selective *in vitro* and *in vivo*, despite the high sequence homology between the CYP11B2/CYP11B1 genes and proteins within a particular species (Roumen, et al., 2007).

A seemingly surprising finding is that MET, a so-called corticosterone inhibitor, was actually several-fold more selective both *in vitro* and *in vivo* for inhibiting CYP11B2 than CYP11B1. Although this lack of CYP11B1 selectivity has been recognized previously (e.g., Gomez-Sanchez, et al., 1997), it does not appear to be widely appreciated. The major reduced metabolites of MET ((+)- and (-)-MOH) (Nagamine, et al., 1997) were unlikely to significantly alter the selectivity profile of MET *in vivo* since both enantiomers exhibited *in vitro* selectivities similar to that of MET itself. However, we estimate that ~80-85% of the PAC- and PCC-lowering effects of therapeutic doses of MET were attributable to these abundant and potent metabolites. In summary, although ~100-300 mg/kg of MET effectively reduced corticosteroid production *in vivo*, MET clearly is not a reliable tool compound for selectively attenuating glucocorticoid production.

Interesting physiologic observations could be gleaned from AS inhibition in our models. For example, the temporal decline of PAC after the highest doses of FAD or MET followed a biphasic pattern similar to the clearance profile of *exogenously* (i.v.) administered radiolabeled aldosterone in rats (fast and slow elimination half-lives of 6 and 36 min, respectively) (Morris, et al., 1975). Based on a bioexponential curve fit to our data, the estimated elimination half-lives of *endogenously* generated aldosterone were 8 and 66 min, respectively, and independent of the model or compound. The similar fast phase half-lives (i.e., 8 vs. 6 min) indicate rapid drug absorption, distribution to, and inhibition of the target enzyme. The somewhat longer slow-phase half-life may reflect a delayed compensatory upregulation of aldosterone biosynthesis in

response to pharmacologic inhibition of AS, a factor that would not impact the elimination of labeled exogenous aldosterone.

Several limitations of our models can be noted. First, as performed, they do not allow the assessment of a compound's duration of action beyond 8 h. However, the ANG II or ACTH infusion time could readily be extended to achieve this goal. Second, although the primary site of action of these compounds is presumably AS, any off-target inhibition of the ANG II or ACTH signaling pathways or upstream steroidogenic cascade would also affect the PAC/PCC response. Nevertheless, similar responses in both models would rule out possible off-target effects that are specific to either of the two secretagogues' distinct signaling pathways. Likewise, observing an *in vivo* selectivity that is narrower than that predicted by the *in vitro* CYP11B2/CYP11B1 inhibitory profile (e.g., MET in our study) would suggest that the compound also blocks an upstream step common to the mineralocorticoid/glucocorticoid steroidogenic pathways (e.g., cholesterol to pregnenolone). Third, the secretagogues or their biosynthetic products may alter the PK properties of the test compound. For example, ANG II (but not ACTH) is a potent vasoconstrictor that can alter renal or liver blood flow and, therefore, the elimination/metabolism profile of the ASI.

In spite of these modest limitations, our two models demonstrate utility for robustly and simultaneously assessing the PK/PD profiles of test compounds. When combined with *in vitro* rat and human data, the models can be used to identify selective and effective clinical ASI candidates such as FAD. These agents are expected to be novel treatments for diseases such as hyperaldosteronism, resistant hypertension, and heart failure.

### **ACKNOWLEDGMENTS**

The authors thank Drs. Gary Ksander and Jim Zhou for preparing, separating, and conducting the optical rotation analysis of the MOH enantiomers, Ye Lu, Jakal Amin, Shaoyong Li, and Wieslawa Maniara for their skillful bioanalytic/PK assistance, and Drs. Keith DiPetrillo, Gary Ksander, and Joel Menard for their valuable feedback on the manuscript.

## REFERENCES

Brandish PE, Chen H, Szczerba P and Hershey JC (2008) Development of a simplified assay for determination of the antiminerlocorticoid activity of compounds dosed in rats. *J Pharmacol Toxicol Methods* **57**:155-160.

Carballeira A, Cheng SC and Fishman LM (1974) Sites of metyrapone inhibition of steroid biosynthesis by rat adrenal mitochondria. *Acta Endocrinol (Copenh)* **76**:703-711.

Cohn JN and Colucci W (2006) Cardiovascular effects of aldosterone and post-acute myocardial infarction pathophysiology. *Am J Cardiol* **97**:4F-12F.

Connell JMC and Davies E (2005) The new biology of aldosterone. *J Endocrinol* **186**:1-20.

Dowsett M, Stein RC, Mehta A and Coombes RC (1990) Potency and selectivity of the nonsteroidal aromatase inhibitor CGS16949A in postmenopausal breast-cancer patients. *Clin Endocrinol (Oxf)* **32**:623-634.

Fiebeler A, Muller DN, Shagdarsuren E and Luft FC (2007) Aldosterone, mineralocorticoid receptors, and vascular inflammation. *Curr Opin Nephrol Hypertens* **16**:134-142.

Fiebeler A, Nussberger JR, Shagdarsuren E, Rong S, Hilfenhaus G, Al-Saadi N, Dechend R, Wellner M, Meiners S, Maser-Gluth C, Jeng AY, Webb RL, Luft FC and Muller DN (2005)

Aldosterone synthase inhibitor ameliorates angiotensin II-induced organ damage. *Circulation* **111**:3087-3094.

Funder JW (2009) Reconsidering the roles of the mineralocorticoid receptor. *Hypertension* **53**:286-290.

Funder JW (2006) Eplerenone: hypertension, heart failure and the importance of mineralocorticoid receptor blockade. *Future Cardiol* **2**:535-541.

Garnier A, Bendall JK, Fuchs S, Escoubet B, Rochais F, Hoerter J, Nehme J, Ambroisine ML, De Angelis N, Morineau G, d'Estienne P, Fischmeister R, Heymes C, Pinet F and Delcayre C (2004) Cardiac specific increase in aldosterone production induces coronary dysfunction in aldosterone synthase-transgenic mice. *Circulation* **110**:1819-1825.

Gomez-Sanchez CE, Zhou MY, Cozza EN, Morita H, Foecking MF and Gomez-Sanchez EP (1997) Aldosterone biosynthesis in the rat brain. *Endocrinology* **138**:3369-3373.

Komor J and Muller J (1979) Effects of prolonged infusions of potassium-chloride, adrenocorticotropin or angiotensin-II upon serum aldosterone concentration and the conversion of corticosterone to aldosterone in rats. *Acta Endocrinol (Copenh)* **90**:680-691.

LaSala D, Shibasaki Y and Jeng AY (2009) Coexpression of CYP11B2 or CYP11B1 with adrenodoxin and adrenodoxin reductase for assessing the potency and selectivity of aldosterone synthase inhibitors. *Anal Biochem* **394**:56-61.

Lea WB, Kwak ES, Luther JM, Fowler SM, Wang Z, Ma J, Fogo AB and Brown NJ (2009) Aldosterone antagonism or synthase inhibition reduces end-organ damage induced by treatment with angiotensin and high salt. *Kidney Int* **75**:936-944.

Makhanova N, Hagaman J, Kim HS and Smithies O (2008) Salt-sensitive blood pressure in mice with increased expression of aldosterone synthase. *Hypertension* **51**:134-140.

Marney AM and Brown NJ (2007) Aldosterone and end-organ damage. *Clin Sci* **113**:267-278.

Mazzocchi G, Rebuffat P, Meneghelli V and Nussdorfer GG (1989) Effects of the infusion with ACTH or CRH on the secretory activity of rat adrenal cortex. *J Steroid Biochem* **32**:841-843.

McManus F, McInnes GT and Mc Connell J (2008) Drug insight: eplerenone, a mineralocorticoid-receptor antagonist. *Nat Clin Pract Endocrinol Metab* **4**:44-52.

Menard J, Gonzalez MF, Guyene TT and Bissery A (2006) Investigation of aldosterone-synthase inhibition in rats. *J Hypertens* **24**:1147-1155.

Menard J and Pascoe L (2006) Can the dextroenantimer of the aromatase inhibitor fadrozole be useful for clinical investigation of aldosterone-synthase inhibition? *J Hypertens* **24**:993-997.

Minnaard-Huiban M, Emmen JMA, Roumen L, Beugels IPE, Cohuet GMS, van Essen H, Ruijters E, Pieterse K, Hilbers PAJ, Ottenheijm HCJ, Plate R, de Gooyer ME, Smits JFM and Hermans JJR (2008) Fadrozole reverses cardiac fibrosis in spontaneously hypertensive heart failure rats: discordant enantioselectivity versus reduction of plasma aldosterone. *Endocrinology* **149**:28-31.

Morris DJ, Graham WC and Davis RP (1975) Metabolism and Binding Properties of H-3 Aldosterone in plasma and its sex dependence in adrenalectomized rats. *Endocrinology* **96**:178-184.

Mulder P, Mellin V, Favre J, Vercauteren M, Remy-Jouet I, Monteil C, Richard V, Renet S, Henry JP, Jeng AY, Webb RL and Thuillez C (2008) Aldosterone synthase inhibition improves cardiovascular function and structure in rats with heart failure: a comparison with spironolactone. *Eur Heart J* **29**:2171-2179.

Muller-Vieira U, Angotti M and Hartmann RW (2005) The adrenocortical tumor cell line NCI-H295R as an in vitro screening system for the evaluation of CYP11B2 (aldosterone synthase) and CYB11B1 (steroid-11 beta-hydroxylase) inhibitors. *J Steroid Biochem Mol Biol* **96**:259-270.



Nagamine S, Horisaka E, Fukuyama Y, Maetani K, Matsuzawa R, Iwakawa S and Asada S (1997) Stereoselective reductive metabolism of metyrapone and inhibitory activity of metyrapone metabolites, metyrapol enantiomers, on steroid 11 beta-hydroxylase in the rat. *Biological & Pharmaceutical Bulletin* **20**:188-192.

Perschel FH, Schemer R, Seiler L, Reincke M, Deinum J, Maser-Gluth C, Mechelhoff D, Tauber R and Diederich S (2004) Rapid screening test for primary hyperaldosteronism: ratio of plasma aldosterone to renin concentration determined by fully automated chemiluminescence immunoassays. *Clin Chem* **50**:1650-1655.

Phillips JL, Walther MM, Pezzullo JC, Rayford W, Choyke PL, Berman AA, Lineman WM, Doppman JL and Gill JR (2000) Predictive value of preoperative tests in discriminating bilateral adrenal hyperplasia from an aldosterone-producing adrenal adenoma. *J Clin Endocrinol Metab* **85**:4526-4533.

Pitt B, Zannad F, Remme WJ, Cody R, Castaigne A, Perez A, Palensky J and Wittes J (1999) The effect of spironolactone on morbidity and mortality in patients with severe heart failure. *N Engl J Med* **341**:709-717.

Rocha R and Funder JW (2002) The pathophysiology of aldosterone in the cardiovascular system. *Endocr Hypertens* **970**:89-100.

Roesch DM, Tian Y, Verbalis JG and Sandberg K (2000) Rat model for investigating ACTH-independent angiotensin-induced aldosterone secretion. *J Renin Angiotensin Aldosterone Syst* **1**:36-39.

Roumen L, Sanders MPA, Pieterse K, Hilbers PAJ, Plate R, Custers E, de Gooyer M, Smits JFM, Beugels I, Emmen J, Ottenheijm HCJ, Leysen D and Hermans JJR (2007) Construction of 3D models of the CYP11B family as a tool to predict ligand binding characteristics. *J Comput Aided Mol Des* **21**:455-471.

Rowland NE and Morian KR (1999) Roles of aldosterone and angiotensin in maturation of sodium appetite in furosemide-treated rats. *American Journal of Physiology-Regulatory Integrative and Comparative Physiology* **276**:R1453-R1460.

Rudolph AE, Rocha R and McMahon EG (2004) Aldosterone target organ protection by eplerenone. *Mol Cell Endocrinol* **217**:229-238.

Sander M, Bader M, Djavidani B, Masergluth C, Vecsel P, Mullins J, Ganten D and Peters J (1992) The role of the adrenal-gland in hypertensive transgenic rat TGR(mREN2)27. *Endocrinology* **131**:807-814.

Siragy HM and Xue C (2008) Local renal aldosterone production induces inflammation and matrix formation in kidneys of diabetic rats. *Exp Physiol*.

Stein RC, Dowsett M, Davenport J, Hedley A, Ford HT, Gazet JC and Coombes RC (1990) Preliminary study of the treatment of advanced breast cancer in postmenopausal women with the aromatase inhibitor CGS16949A. *Cancer Res* **50**:1381-1384.

Trunet PF, Mueller P, Girard F, Aupetit B, Bhatnagar AS, Zognbi F, Ezzet F and Menard J (1992) The effects of fadrozole hydrochloride on aldosterone secretion in healthy male-subjects. *J Clin Endocrinol Metab* **74**:571-576.

Unger N, Schmidt IL, Pitt C, Walz MK, Philipp T, Mann K and Petersenn S (2004) Comparison of active renin concentration and plasma renin activity for the diagnosis of primary hyperaldosteronism in patients with an adrenal mass. *Euro J Endocrinol* **150**:517-523.

Weber KT (2001) Mechanisms of disease - Aldosterone in congestive heart failure. *N Engl J Med* **345**:1689-1697.

Ye P, Kenyon CJ, MacKenzie SM, Seckl JR, Fraser R, Connell JMC and Davies E (2003) Regulation of aldosterone synthase gene expression in the rat adrenal gland and central nervous system by sodium and angiotensin II. *Endocrinology* **144**:3321-3328.

## FOOTNOTES

Footnote to title: This study was funded by Novartis Pharmaceuticals Corporation.

Address for reprint requests:

Dr. Dean F. Rigel

One Health Plaza

Building 437/3321

Novartis Institutes for BioMedical Research

Novartis Pharmaceuticals Corporation

East Hanover, NJ 07936-1080

[dean.rigel@novartis.com](mailto:dean.rigel@novartis.com)

## LEGENDS FOR FIGURES

**Fig. 1. *In vitro* concentration-response relationships for FAD, MET, (+)-MOH, and (-)-MOH.** Various concentrations of the compounds were incubated for 4 h at 25°C with homogenized adrenal capsular tissue from rats and the substrate 11-deoxycorticosterone. CYP11B1 and CYP11B2 activities were assessed by measuring generated corticosterone or aldosterone, respectively. All four compounds dose-dependently inhibited biosynthesis of the two steroids. IC<sub>50</sub> values (Table 1) were estimated by fitting the individual concentration-response data to a four-parameter sigmoidal model.

**Fig. 2. Time courses of PAC and PCC in the ANG II- and ACTH- infused rats (controls).** Conscious chronically cannulated rats were infused i.v. with ANG II (300 ng/kg bolus + 100 ng/kg/min; upper panel) or ACTH (100 ng/kg bolus + 30 ng/kg/min; lower panel) for 9 h to increase basal PAC (0.28 nM) and PCC (300 nM) to ~2.5 and ~1300 nM, respectively. At time zero (after 1 h of infusion), rats were administered vehicle (2 ml/kg water, p.o.) or left untreated. Results from each control group were similar and, therefore, pooled. Both secretagogues sustained the PAC increases for the duration of the experiment whereas only ACTH maintained the PCC increase. Values (n=11 (ANG II) and 8 (ACTH) rats) represent the mean (± SEM) PAC or PCC expressed as a percent of the respective baseline (time zero) value. \*Significantly different from baseline (100%) by one-way ANOVA and Dunnett's test.

**Fig. 3. Time courses of PAC and plasma concentrations of FAD and MET in the ANG II model.** Procedures followed those described in Fig. 2 except that rats were administered FAD (0.01-30 mg/kg p.o.) or MET (0.1-100 mg/kg p.o.) at time zero. Values (n=3-5 rats per treatment group) represent the mean (± SEM) PAC expressed as a percent of baseline (upper panels) or total plasma concentrations of FAD and MET (lower panels).

**Fig. 4. Time courses of PAC, PCC, and plasma concentrations of FAD and MET in the ACTH model.** Procedures followed those described in Fig. 2 except that rats were administered FAD (0.03-100 mg/kg p.o.) or MET (0.3-300 mg/kg p.o.) at time zero. Values (n=3-5 rats per treatment group) represent the mean ( $\pm$  SEM) PAC expressed as a percent of baseline (upper panels), PCC expressed as a percent of baseline (middle panels), or total plasma concentrations of FAD and MET (lower panels).

**Fig. 5. Dose-response relationships for FAD and MET in the ANG II and ACTH models.** Procedures followed those described in Fig. 2 except that rats were administered FAD (0.01-100 mg/kg p.o.) or MET (0.1-300 mg/kg p.o.) at time zero. Results (mean  $\pm$  SEM; n=3-5 rats per treatment group) are expressed as the peak (upper panels) and 8-h TWA (lower panels) PAC or PCC as a percent of the respective baseline value for each rat. Only PAC was evaluated in the ANG II model whereas both PAC and PCC were assessed in the ACTH model. Grey symbols represent the control (C) responses depicted in Fig. 2.

**Fig. 6. Dose-exposure relationships for FAD and MET in the ANG II and ACTH models.** Procedures followed those described in Fig. 2 except that rats were administered FAD (0.01-100 mg/kg p.o.) or MET (0.1-300 mg/kg p.o.) at time zero. Results (mean  $\pm$  SEM; n=3-5 rats per treatment group) are expressed as the peak (upper panels) and 8-h TWA (lower panels) total plasma concentrations of FAD and MET for the two models. In rats treated with 0.01 mg/kg FAD, most of the plasma concentrations were below the quantification limit. Peak MET concentrations after i.a. administration in both models are almost identical; therefore, the two symbols are superimposed. Plasma protein binding for FAD and MET was 57% and 33%, respectively. Thus, the unbound concentrations of FAD and MET were 43% and 67%, respectively, of the indicated values.

**Fig. 7. FAD and MET plasma exposure-response relationships in the ANG II and ACTH models.** Dose-response (Fig. 5) and dose-exposure (Fig. 6) relationships for FAD or MET were combined to generate the respective peak (upper panels) and 8-h TWA (lower panels) drug-exposure-response relationships for PAC and PCC in the two models. Grey symbols represent the control (C) responses depicted in Fig. 2. Values are mean  $\pm$  SEM (n=3-5 rats per treatment group).

**TABLE 1**

**IC<sub>50</sub> values of compounds for inhibiting the production of aldosterone and corticosterone in an *in vitro* rat adrenal cortical preparation**

Values were derived by fitting the individual concentration-response data in Fig. 1 to a 4-parameter sigmoidal dose-response model.

|         | IC <sub>50</sub> (nM) |                | Selectivity <sup>a</sup> |
|---------|-----------------------|----------------|--------------------------|
|         | Aldosterone           | Corticosterone |                          |
| FAD286  | 670                   | 3400           | 5                        |
| MET     | 890                   | 1400           | 2                        |
| (+)-MOH | 700                   | 2500           | 4                        |
| (-)-MOH | 4500                  | 3100           | 1                        |

<sup>a</sup>Ratios of the IC<sub>50</sub> values for inhibiting corticosterone and aldosterone production (i.e., CYP11B2/CYP11B1 selectivity).



**TABLE 2**

**ED<sub>50</sub> and EC<sub>50</sub> values of compounds for lowering PAC and PCC in the *in vivo* Ang II and ACTH models**

Values were derived by fitting the composite dose-response data in Fig. 5 or the exposure-response data in Fig. 7 to a 4-parameter sigmoidal dose-response model.

|                     | ED <sub>50</sub> (mg/kg p.o.) |     |                                  | EC <sub>50</sub> (nM) |      |                      |      |                                  |
|---------------------|-------------------------------|-----|----------------------------------|-----------------------|------|----------------------|------|----------------------------------|
|                     | PAC                           | PCC | <sup>a</sup> PAC/PCC selectivity | Total                 |      | <sup>b</sup> Unbound |      | <sup>a</sup> PAC/PCC selectivity |
|                     |                               |     |                                  | PAC                   | PCC  | PAC                  | PCC  |                                  |
| <u>Ang II model</u> |                               |     |                                  |                       |      |                      |      |                                  |
| FAD                 | 0.5                           | --  | --                               | 120                   | --   | 54                   | --   | --                               |
| MET                 | 5.5                           | --  | --                               | 120                   | --   | 82                   | --   | --                               |
| <u>ACTH model</u>   |                               |     |                                  |                       |      |                      |      |                                  |
| FAD                 | 0.8                           | 45  | 54                               | 480                   | 2300 | 210                  | 1000 | 48                               |
|                     |                               |     |                                  |                       | 0    |                      | 0    |                                  |
| MET                 | 10.6                          | 40  | 4                                | 1300                  | 3600 | 880                  | 2500 | 3                                |

<sup>a</sup>Ratios of the ED<sub>50</sub> (or EC<sub>50</sub>) values for lowering PCC and PAC.

<sup>b</sup>Unbound exposures are estimated by the *in vitro* plasma protein binding values (see text).

**TABLE 3**

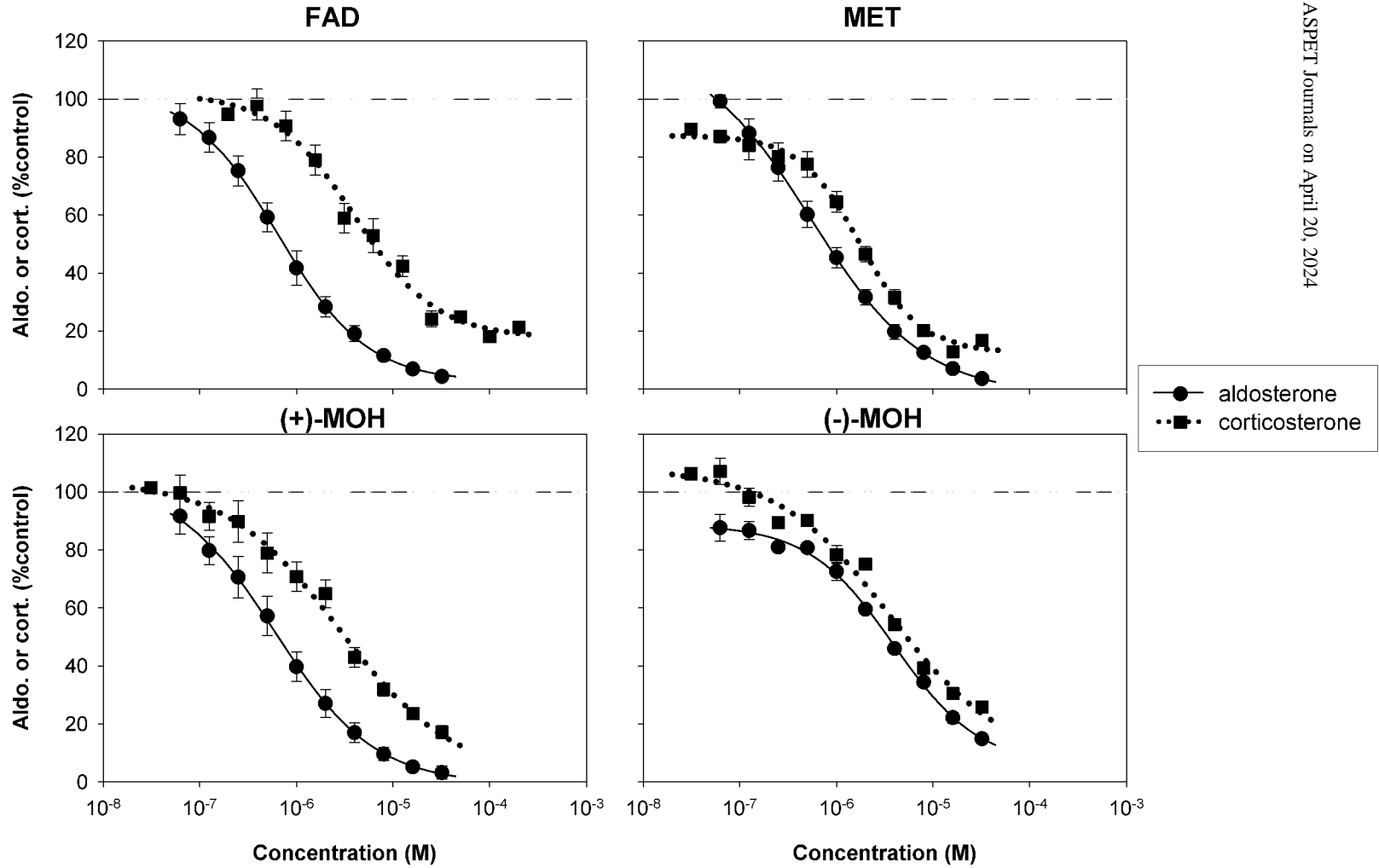
**Pharmacokinetic parameters of FAD and MET in the *in vivo* Ang II and ACTH models**

| Parameter       | FAD                   |                       | MET             |                 |
|-----------------|-----------------------|-----------------------|-----------------|-----------------|
|                 | Ang II                | ACTH                  | Ang II          | ACTH            |
| $t_{1/2}$ (h)   | $3.8 \pm 0.8$         | $\dagger 3.2 \pm 0.4$ | $10.0 \pm 2.6$  | $6.8 \pm 0.2$   |
| CL (l/h/kg)     | $*0.42 \pm 0.05$      | $0.78 \pm 0.12$       | $0.52 \pm 0.02$ | $0.44 \pm 0.04$ |
| $V_{ss}$ (l/kg) | $\dagger 1.5 \pm 0.4$ | $\dagger 2.8 \pm 0.3$ | $7.5 \pm 1.8$   | $4.3 \pm 0.2$   |

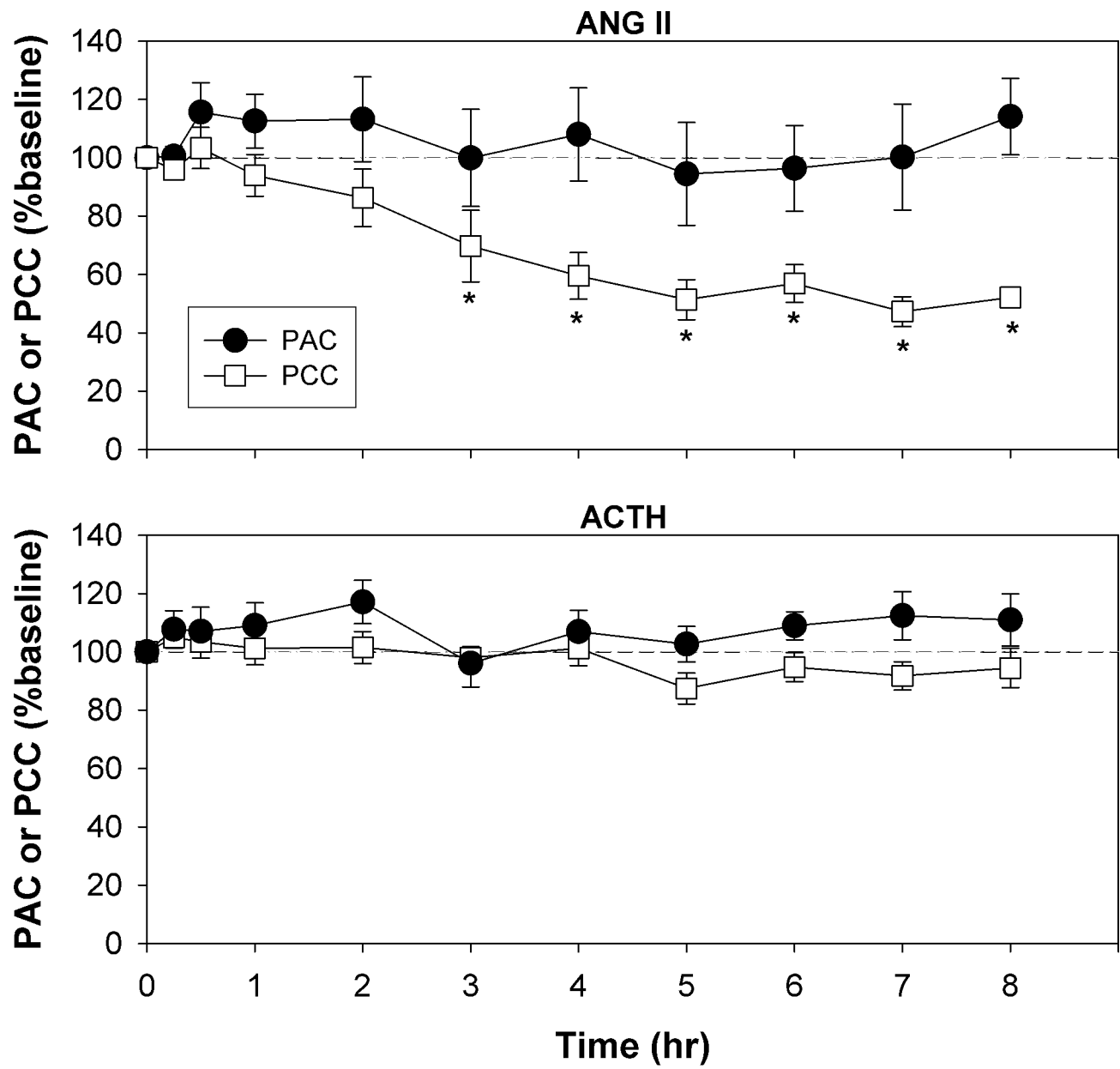
$t_{1/2}$ , terminal elimination half-life; CL, clearance;  $V_{ss}$ , steady-state volume of distribution.

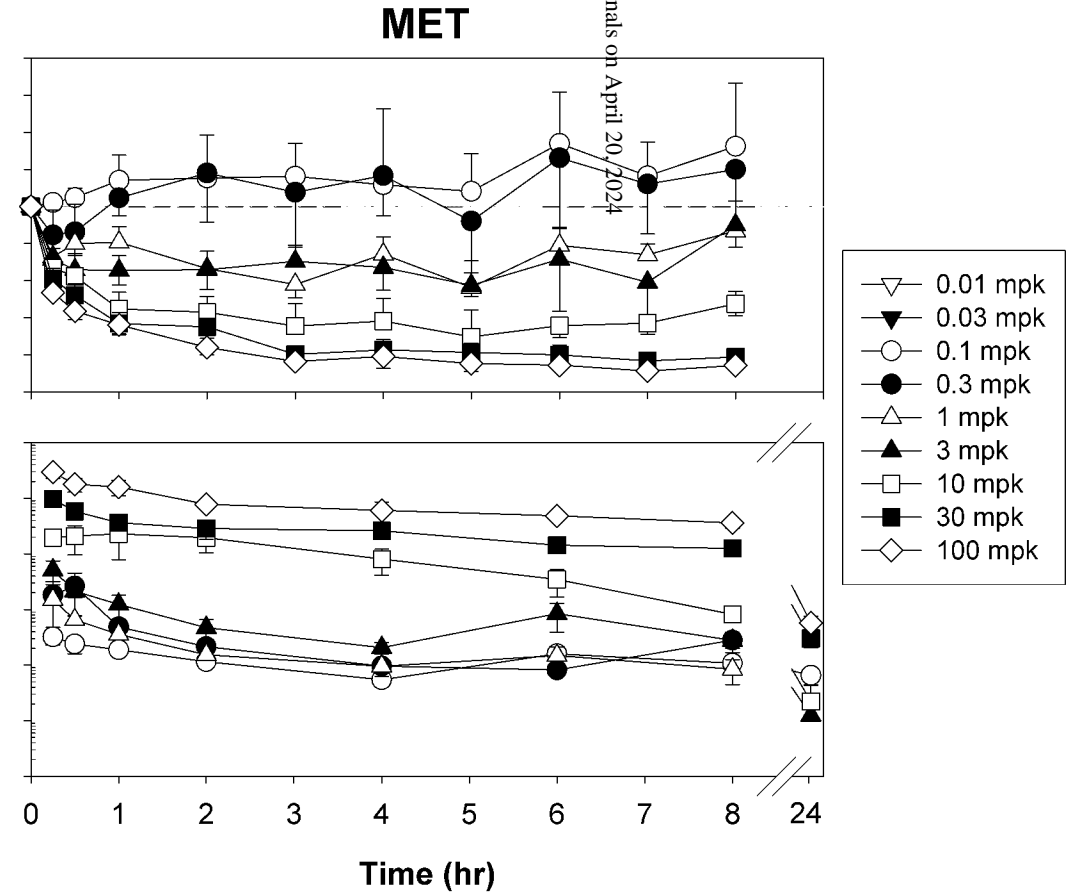
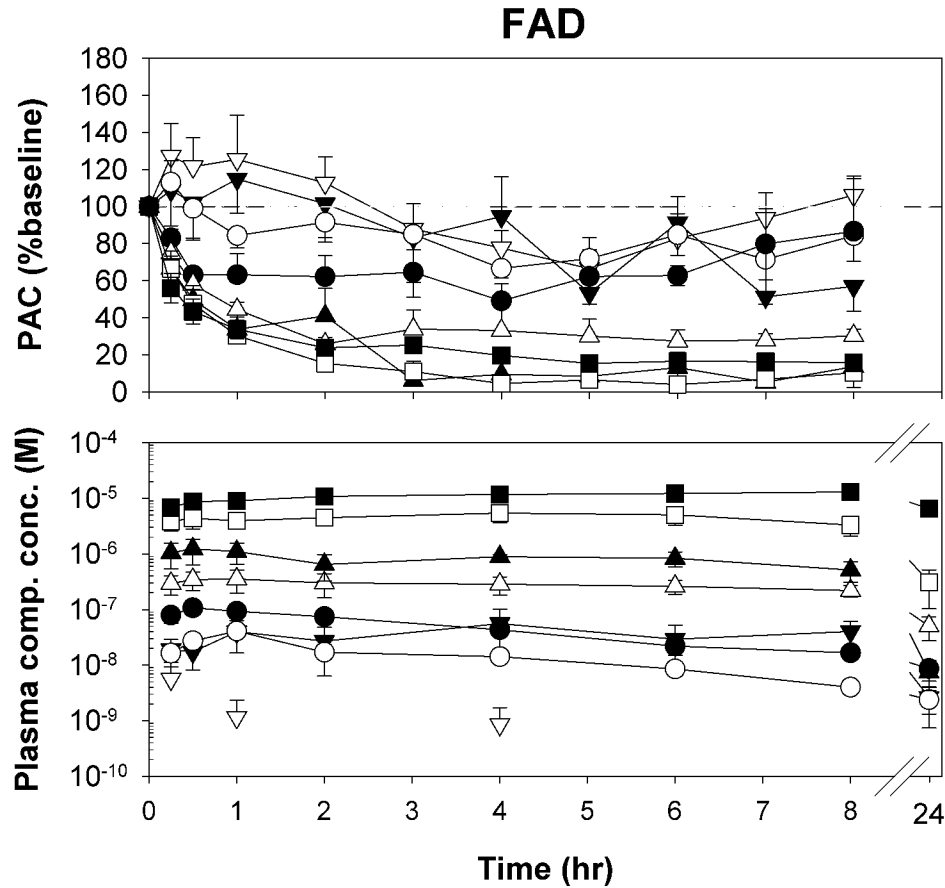
\* $p < 0.05$  vs. FAD in the ACTH model.  $\dagger p < 0.05$  vs. MET in the corresponding model.

**FIGURE 1**

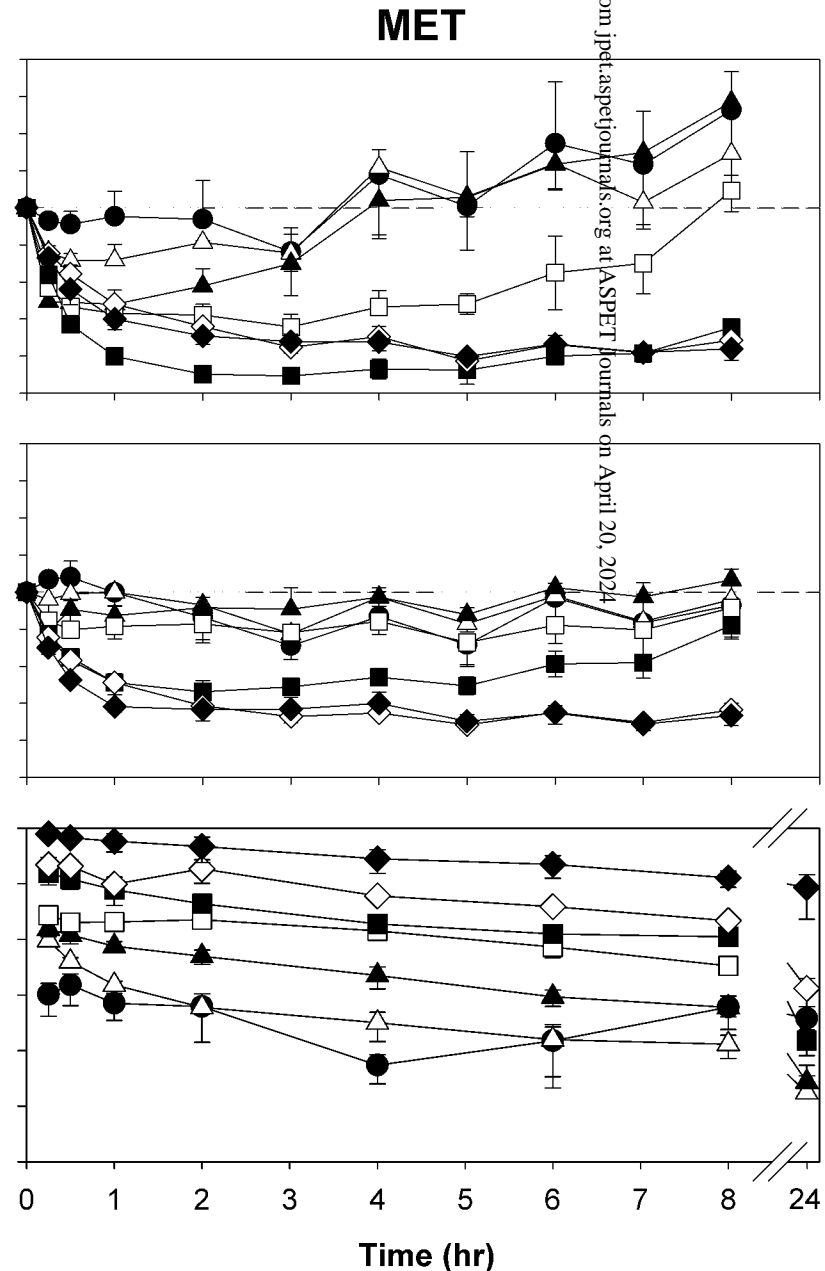
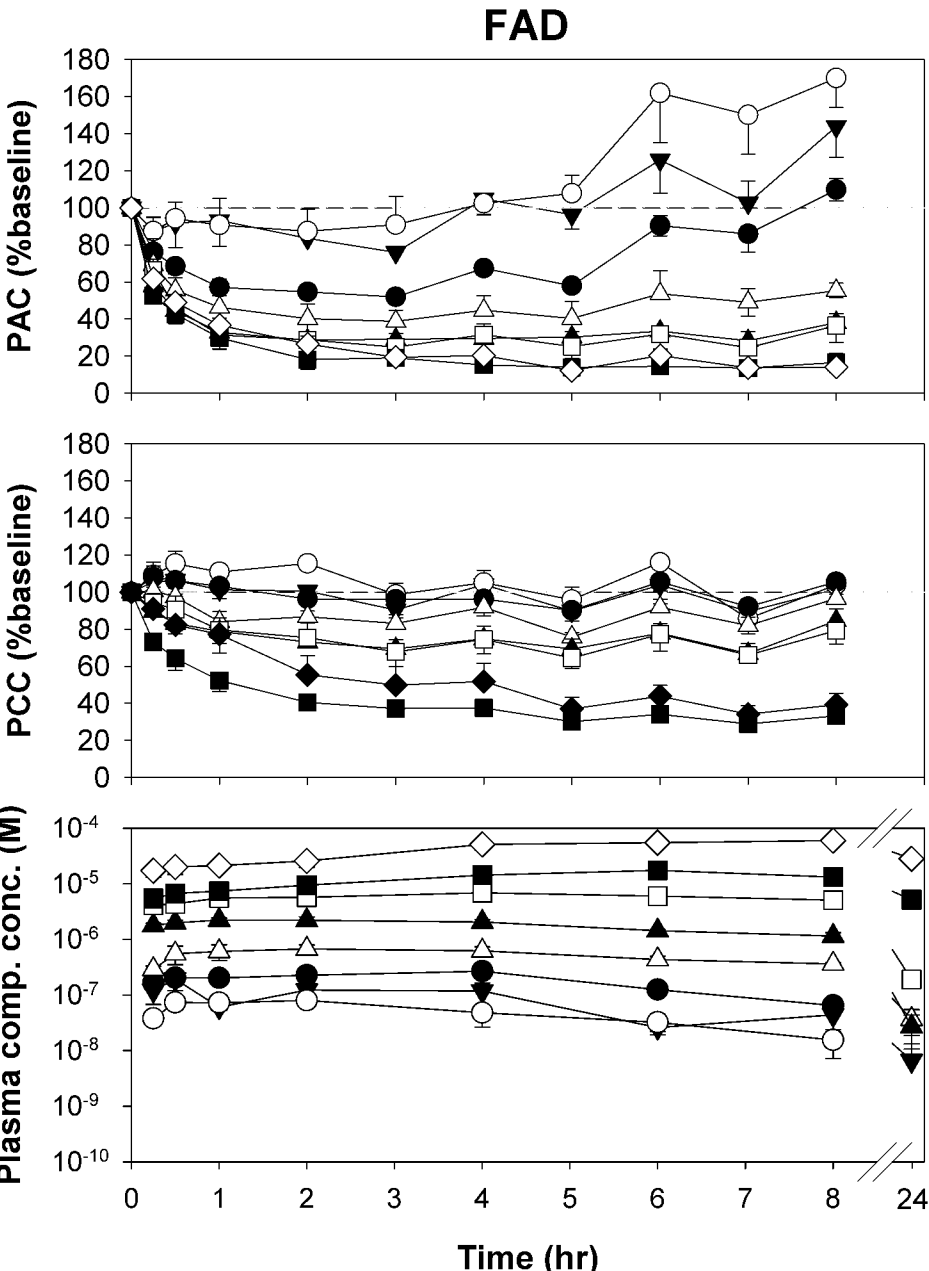


**FIGURE 2**



**FIGURE 3**

**FIGURE 4**



- ▼ 0.03 mpk
- 0.1 mpk
- 0.3 mpk
- △ 1 mpk
- ▲ 3 mpk
- 10 mpk
- 30 mpk
- ◇ 100 mpk
- ◆ 300 mpk

Downloaded from [jpet.aspetjournals.org](http://jpet.aspetjournals.org) at ASPET Journals on April 20, 2024

# FIGURE 5

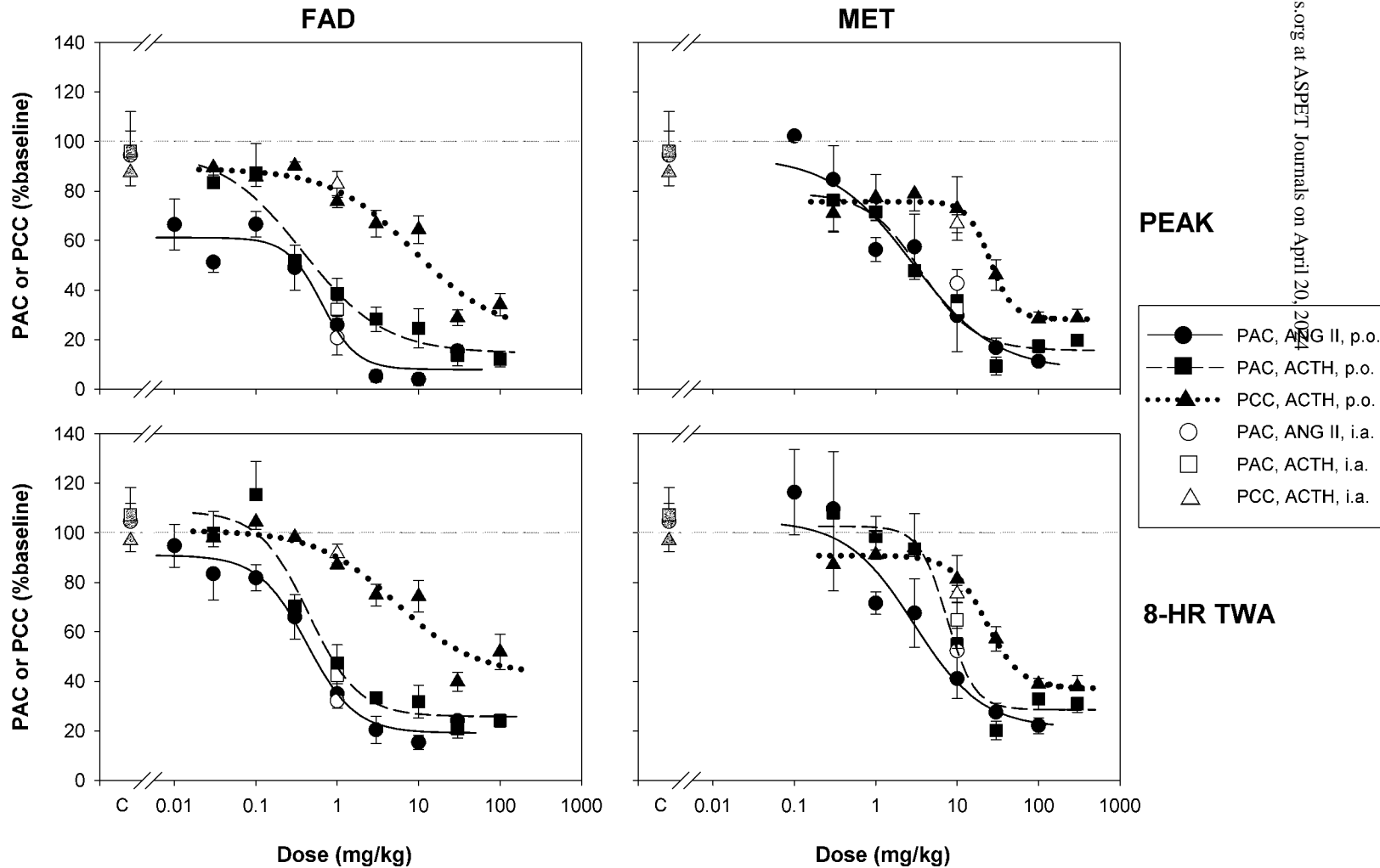


**FIGURE 6**

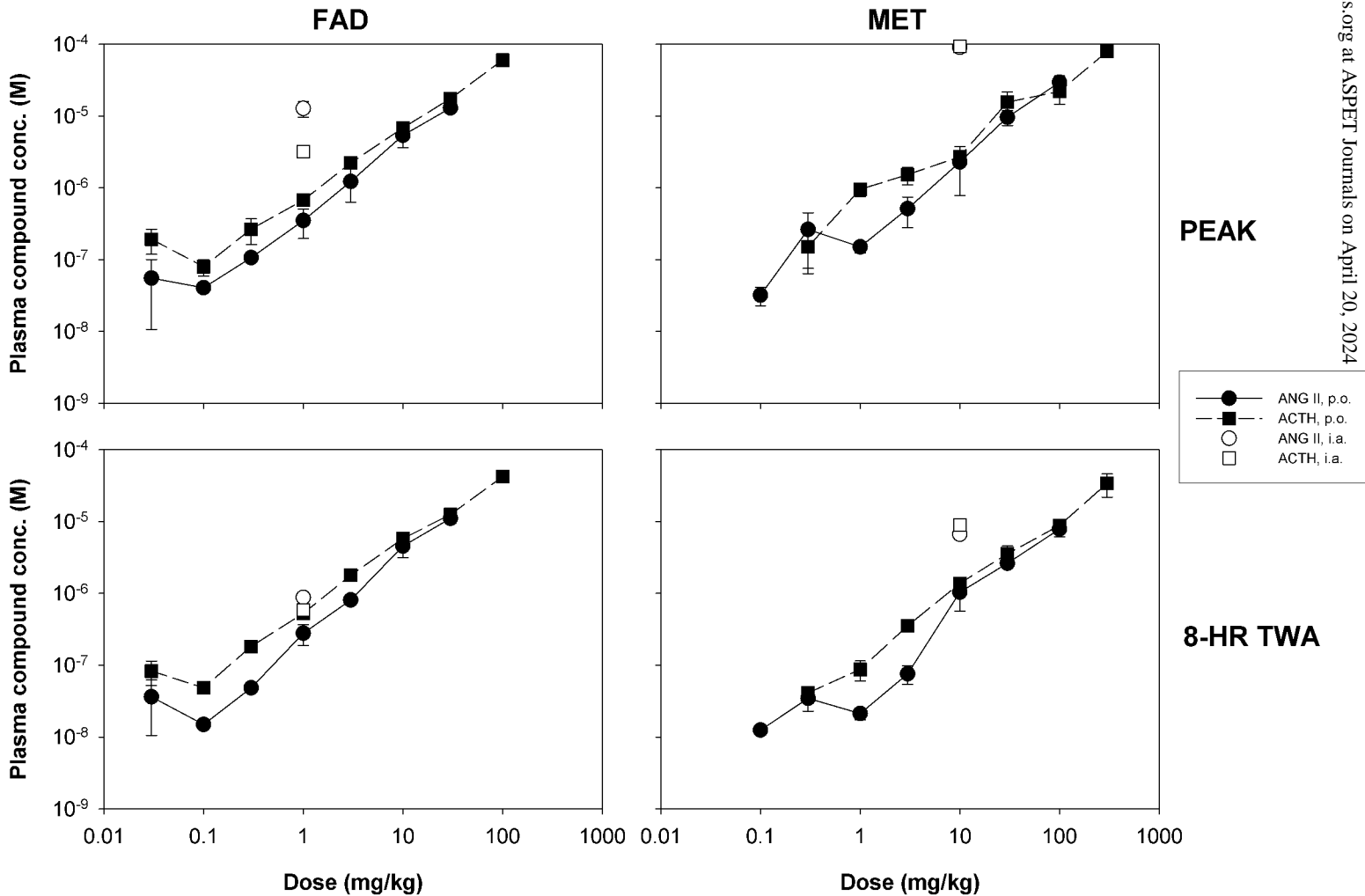




**FIGURE 7**